Journal of Power Sources 240 (2013) 583–588

Contents lists available at SciVerse ScienceDirect

Journal of Power Sources

journal homepage: www.elsevier.com/locate/jpowsour

Transport number measurements and fuel cell testing of undoped and Mo-substituted lanthanum tungstate

Anna Magrasó*

Department of Chemistry, University of Oslo, Centre for Materials Science and Nanotechnology, FERMiO, Gaustadaléen 21, NO-0349 Oslo, Norway

HIGHLIGHTS

- Partial conductivities have been extracted for LWO and Mo-LWO.
- Lanthanum tungstate is suitable as electrolyte for PC-SOFCs.
- Mo-substituted LWO is more suited as membrane material for H_2 gas separation.

ARTICLE INFO

Article history:
Received 4 March 2013
Received in revised form
16 April 2013
Accepted 17 April 2013
Available online 25 April 2013

Keywords:
La_6WO_{12}
$La_{28-x}W_{4+x}O_{54+\delta}$
PC-SOFC
H_2 permeable membrane
Proton conductor
Mixed electron–proton conductor

ABSTRACT

The partial protonic, oxide ion and electronic conductivities of lanthanum tungstate ($La_{28-x}W_{4+x}O_{54+\delta}$ with $x = 1$, LWO54) and 30% molybdenum substituted lanthanum tungstate (Mo-LWO54) have been extracted using the EMF method. LWO54 is a relatively pure ionic conductor up to ~800 °C; above that temperature electrons start to contribute significantly (under reducing conditions). The maximum protonic conductivity is ~2–3 × 10^{-3} S cm^{-1}, and protonic conductivity dominates the ionic regime under wet conditions below ~700 °C. Above this temperature, oxide ion conductivity dominates the ionic contribution. The protonic and oxide ion conductivities for Mo-substituted LWO54 are quite similar to the Mo-free material, while the electronic conductivity is almost one order of magnitude higher for the former in wet 5% H_2/Ar. From this report is clear that nominally undoped lanthanum tungstate is most suited for applications as electrolyte in proton conducting SOFCs, while Mo-LWO54 presents improved mixed proton-electron conductivity for use as dense membrane for hydrogen separation.

1. Introduction

Lanthanum tungstate with the newly proposed stoichiometry $La_{28-x}W_{4+x}O_{54+\delta}v_{2-\delta}$ (earlier on referred as La_6WO_{12}) [1] belongs to a family of materials with very interesting properties for technological applications [2–6]. The nominally undoped material ($0.78 \geq x \geq 1.08$) [6] has inherently vacant oxygen sites (v) that can be hydrated in a similar manner as an acceptor-doped material [7–9]. Lanthanum tungstate (LWO) is a relatively pure proton conducting oxide at low and intermediate temperatures and can therefore be used as electrolyte in proton conducting solid oxide fuel cells (PC-SOFCs) [10,11]. At higher temperatures, the material exhibits additional p-type and n-type electronic conductivity under oxidizing and reducing conditions, respectively. The material can, under reducing conditions, be used as a dense membrane for hydrogen separation *via* ambipolar transport of protons and electrons [12–14]. It has been reported that hydrogen permeation is limited by electrons at all measured temperatures (up to 1000 °C) [12].

It has recently been shown that partial replacement of tungsten by molybdenum in lanthanum tungstate enhances electronic conductivity due to the higher reducibility of Mo compared to W. It was anticipated that the increase in electronic conductivity did not affect the ionic (and protonic) conductivity significantly, so that ambipolar transport would be higher with Mo substitution [15]. Mo-LWO is therefore an improved composition for hydrogen permeation applications compared to LWO.

The transport properties and the defects contributing in lanthanum tungstate and Mo-substituted LWO are relatively well established and understood, but quantification of the partial conductivities of each charge carrier (protons, oxide ions and holes under oxidizing conditions; protons, oxide ions and electrons under reducing conditions) still need to be established. The present contribution will thus focus on the determination of the partial conductivities of each defect using the electromotive force (EMF)

* Tel.: +47 22840660; fax: +47 22840651.
E-mail addresses: a.m.sola@smn.uio.no, annamagraso@gmail.com.

0378-7753/$ – see front matter © 2013 Elsevier B.V. All rights reserved.
http://dx.doi.org/10.1016/j.jpowsour.2013.04.087

generated over a concentration cell [16,17]. The study will be complemented by testing of the performance of electrolyte-supported specimens under fuel cell mode.

2. Experimental section

2.1. Description of the tested samples

Nanometric powders of nominally undoped LWO54 ($La_{27}W_5O_{55.5}$) and 30% Mo-substituted LWO54 (Mo-LWO54; i.e. $La_{27}(W_{0.7}Mo_{0.3})_5O_{55.5}$) were purchased from Cerpotech AS (Trondheim, Norway). The powders were pressed at 100 MPa by uniaxial pressing and the specimens were sintered at 1500 °C for 10 h. The density of the pellets was 98 and 99% of the theoretical for LWO54 and Mo-LWO54, respectively. The samples were single phase materials by X-ray diffraction (Bruker D8, 3-circle diffractometer), in accordance with earlier reports [5,15]. Pt electrodes (Pt ink 6926 from Metalor) were painted on each side of the specimens and fired at 1000 °C for 30 min. The final geometrical factors were the following: area = 0.95 cm^2 and thickness = 0.19 cm (LWO54); area = 0.79 cm^2 and thickness = 0.21 cm (Mo-LWO54).

2.2. Dependency of the conductivity with oxygen and water partial pressure

The conductivity was measured using an Alpha A impedance spectrometer + POTGAL interface (Novocontrol technologies) in a ProboStat™ measurement cell (NorECs, Norway) by the 2-point 4-wire method. Impedance spectra were recorded in the 1 MHz to 0.1 Hz frequency range with an oscillation voltage of 50 mV. The dependence of the conductivity with oxygen partial pressure was measured from O_2 to H_2 at constant pH_2O ($\sim$2.5% H_2O). Typical flow rates are 20–50 ml min^{-1}. The variation of conductivity with water vapor partial pressure was performed in O_2 (oxidizing conditions were chosen in order to minimize the contribution from n-type conductivity for Mo-LWO54). The conductivity was monitored *vs.* time at each new set of conditions to ensure that equilibrium was achieved before taking a measurement.

2.3. Transport number measurements

EMF measurements were performed from 500 to 1000 °C to extract transport numbers using the setup and procedure described in Refs. [16,17]. A thick gold gasket was placed between the specimen and the support tube for sealing, which was accomplished by annealing at $\sim$1060 °C. The open-circuit voltage (OCV) resulting from differences in the gas composition and chemical potentials across the specimen were measured with an Agilent/HP 34401A multimeter. Impedance measurements were conducted under the same gradient in order to correct the transport number (t_i) by electrode polarization, following the suggestion by Liu and Hu [18]:

$$t_i = 1 - \frac{R_b}{R_{tot}}\left(1 - \frac{V_{OC}}{E_N}\right) \quad (1)$$

where R_b and R_{tot} are the material and total resistance deconvoluted from the impedance measurement, and the V_{OC} and E_N are the measured and the Nernst voltage, respectively. The measurements were conducted in both oxidizing (air) and reducing (5% H_2/Ar) conditions to test the consistency of the measurements.

2.4. Fuel cell performance

After the transport numbers were completed, fuel cell performance was recorded using the same setup. The gases were changed to wet air and wet 5% H_2/Ar on either side of the specimens, and the OCV was followed until equilibrium was reached. Then, the cell performance was measured using an Alpha A + POTGAL interface (Novocontrol technologies) on the sealed cell from 500 to 1000 °C. The current–voltage response was collected during 5 s in intervals of 0.1 s under potentiostatic mode from OCV to $\sim$0.1 V in steps of 0.05–0.1 V.

3. Results and discussion

3.1. Measurement of the transport number in mixed ionic-electronic conductors using the EMF method

The total electrical conductivity of a substance is the sum of the partial conductivities of the different charge carriers, and the transport number is the share of conductivity that is due to a species *i*, where the sum of all transport numbers equals unity. In our case, the expression reads:

$$\sum_i t_i = t_{O^{2-}} + t_{H^+} + t_{electronic} = 1 \quad (2)$$

Carl Wagner [19] was the first to combine chemical and electrical potentials and potential gradients to describe the oxidation of metals, and the Wagner-type theory forms the basis for the treatment of all mass transport processes involving charged species in ionic solids. Sutija et al. [20] and Norby [16] derived the expressions for transport number determination by the concentration-cell/open-circuit voltage method for oxides with mixed electronic, ionic and protonic conductivity. When measuring the voltage under a gradient in partial pressure of O_2 (pH_2O must be kept constant), the voltage under the assumptions and simplifications described in Refs [16,17] can be described as:

$$E_{II-I} = t_{ion}\frac{RT}{4F}\ln\left(\frac{P^{II}_{O_2}}{P^{I}_{O_2}}\right) \quad (3)$$

where t_{ion} denotes the sum of transport number for ionic species (protons and oxide ions in this case) and E_{II-I} refers to the measured voltage under the given gradient I and II. Other entities have their usual meanings. When the voltage is measured under a gradient of partial pressure of H_2O (pO_2 must be kept constant), the corresponding Nernst equation may be derived in terms of the oxygen and water partial pressures:

$$E_{II-I} = t_{H^+}\cdot\frac{RT}{2F}\ln\left(\frac{P^{II}_{O_2}}{P^{I}_{O_2}}\right) - t_{H^+}\cdot\frac{RT}{2F}\ln\left(\frac{P^{II}_{H_2O}}{P^{I}_{H_2O}}\right) \quad (4)$$

When t_{ion} and t_{H^+} are determined, $t_{O^{2-}}$ and $t_{electronic}$ can be easily calculated using $t_{ion} = t_{O^{2-}} + t_{H^+}$ and equation (2). It is worth to mention that, in the present contribution, several OCVs have been measured per each set of conditions (temperature and either pH_2O or pO_2) and the given t_i is the transport number extrapolated to zero gradient as reported in Refs. [21], in order to satisfy one of the assumptions of equations (3) and (4). A representative example is given in Fig. 1. Typical gas conditions under oxidizing and reducing conditions are displayed in Table 1.

3.2. Transport number measurements of LWO54 and Mo-LWO54

Fig. 2 displays the variation of the conductivity with the oxygen partial pressure (pO_2) and shows the behavior of a mixed ionic-electronic conductor. The conductivity is independent of the pO_2 at intermediate pressures, indicating dominating ionic conductivity. At high temperatures and high pO_2, the conductivity increases with increasing the pO_2, indicating the presence of p-type

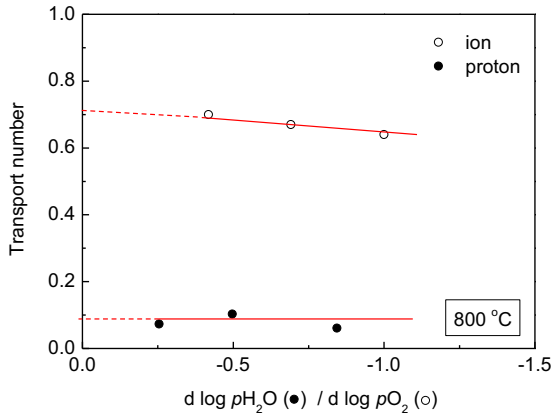

Fig. 1. Transport number of ions *vs.* gradient in oxygen partial pressure in air + Ar mixtures under wet conditions (empty circles) and transport number of protons *vs.* gradient in water vapor partial pressure gradient in wet air + dry air mixtures. The temperature is 800 °C and the composition is LWO54.

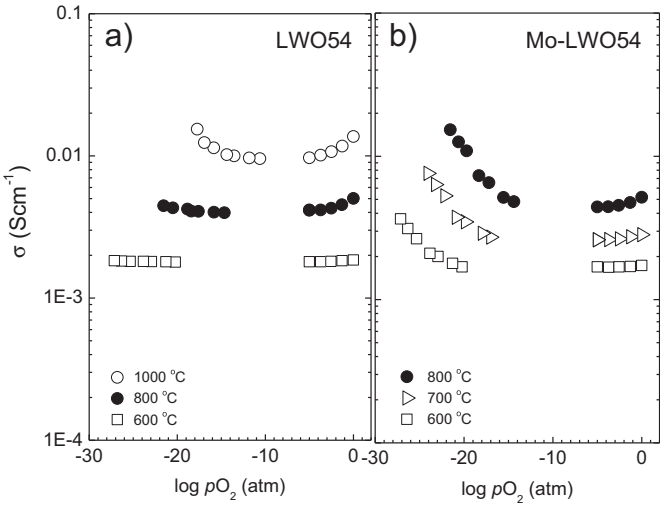

Fig. 2. Variation of the conductivity with oxygen partial pressure from H_2 to O_2 for a) LWO54 and b) Mo-LWO54 in wet conditions.

conductivity. At high temperatures and low pO_2, the conductivity increases with decreasing pO_2, which is consistent with n-type conductivity. The effect of Mo-substitution in lanthanum tungstate is clear: there is a strong enhancement of the n-type electronic conductivity for the composition with Mo, while the p-type and ionic conductivity remains almost unaffected, as shown earlier [15]. The variation of the conductivity with pH_2O (see Fig. 3) shows that the dependency for both LWO54 and Mo-LWO54 is similar, indicating that they present similar proton conductivities. The transport numbers described in the following paragraph will confirm this statement.

The "apparent" t_{ion} measured under oxidizing conditions decreases with increasing temperature for both LWO54 and Mo-LWO54. This is not in accordance with the transport properties of these materials, and this phenomenon is ascribed to the influence of the electrodes. It is well known that good ionic conductors present high polarization resistances with Pt, and this effect is most pronounced at low temperatures. The electrode interface is much less resistive under reducing conditions (see Fig. 4 for a representative Nyquist plot), and the apparent t_{ion} under reducing conditions at the lowest temperatures is higher than under oxidizing conditions. The transport numbers have, therefore, been corrected by the electrode polarization, as suggested in Ref. [18], and only the corrected t_i will be discussed further in the manuscript.

The transport number of ions (protons and oxide ions) under oxidizing conditions increases slightly from ~0.9 (900 °C) to ~1 (500 °C) for both LWO54 and Mo-LWO54, confirming that the main charge carriers are ions, and that electron holes contribute only at relatively high temperatures. On the other hand, t_{H^+} clearly increases with decreasing temperature from ~0.4 (at 900 °C) to ~1 (500 °C). This means that protons increase their dominance over oxide ions toward low temperatures, as expected from the exothermic nature of the hydration reaction:

$$H_2O + v_O^{\bullet\bullet} + O_O^x = 2OH_O^{\bullet} \quad (5)$$

It is worth to highlight that the transport properties of LWO54 and Mo-LWO54 under oxidizing conditions are essentially equal, as anticipated earlier [15]. The dependency of conductivity with pO_2 and pH_2O is comparable for both materials (c.f. Figs. 2 and 3), so this behavior is expected.

The transport number of ions (protons and oxide ions) and protons for LWO54 under reducing conditions are quite comparable to those extracted from oxidizing conditions. This is in accordance with the variation of the conductivity with pO_2 in Fig. 2a: the dependency for LWO54 is quite symmetric, indicating that electrons and electron holes contribute in equal amounts to the conductivity in wet 5% H_2/Ar (reducing) and wet air (oxidizing) conditions, respectively. The transport properties of Mo-LWO54 under reducing conditions are different than for oxidizing conditions: t_{ion} decreases significantly with increasing temperature, where electrons contribute more. This confirms that Mo substitution in LWO54 increases the electronic conductivity to a large extent, in accordance with [15].

The partial protonic, oxide ion and electronic conductivities for LWO54 and Mo-LWO54 calculated from the corrected transport numbers in 5% H_2/Ar are displayed in Fig. 5. They show a typical behavior of mixed electron-proton conducting oxides: at low temperatures and wet conditions, protonic conductivity dominates and the material behaves as an essentially pure protonic conductor. At intermediate temperatures (~700 °C), the material starts to dehydrate, looses protons and forms oxygen vacancies (cf. equation (5)) and oxide ion conductivity starts to contribute significantly. At the highest temperatures, electrons also contribute to the total conductivity. One may be reminded here that separating the

Table 1
Summary of experimental conditions to extract the transport numbers. Harmix = 5% H_2/Ar.

To extract	*Gas 1*	*Gas 2*	pH_2O(I) (atm)	pH_2O(II) (atm)	pO_2(I) (atm)	pO_2(II) (atm)
Oxidizing conditions						
t_{ion}	Wetted air	Wetted (air + Ar)	0.023	0.023	0.21	0.01–0.2
t_{H^+}	Wetted air	Dry air + wetted air	0.023	0.002–0.02	0.21	0.21
Reducing conditions						
t_{ion}	Wetted harmix	Wetted (harmix + Ar)	0.023	0.023	1×10^{-19}, [a]	5×10^{-17}–5×10^{-19}, [a]
t_{H^+}	Wetted air	(Wetted harmix) + Ar	0.023	0.004–0.02	1×10^{-19}, [a]	1×10^{-19}, [a]

[a] The oxygen partial pressure under reducing conditions depends on temperature. Here, 800 °C is given as example.

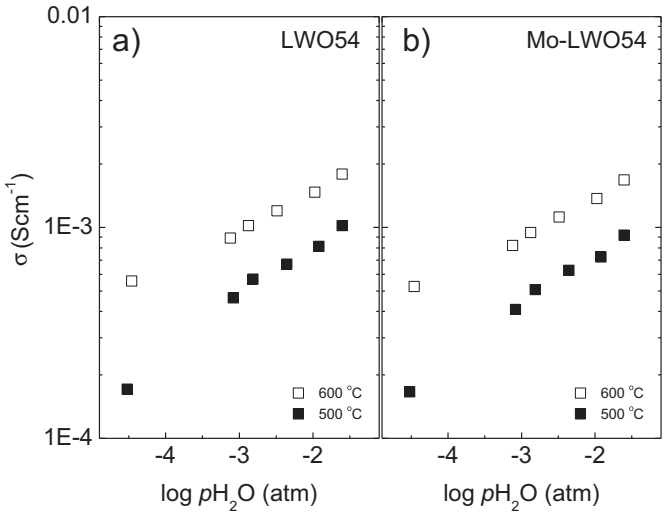

Fig. 3. Dependence of the conductivity with water vapor partial pressure for a) LWO54 and b) Mo-LWO54 at 500 and 600 °C in O_2.

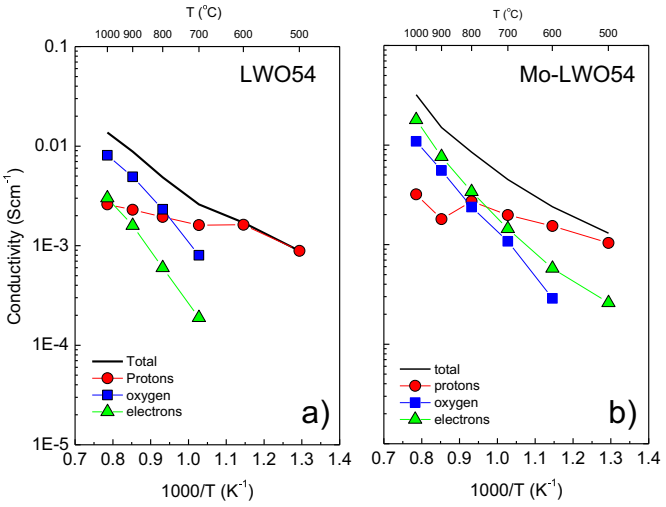

Fig. 5. Partial and total conductivities in 5% H_2/Ar for (a) LWO54 and (b) Mo-LWO54.

contribution of each species in a region where 3 different defects contribute simultaneously may not render "exact" partial conductivities, especially when the correction by polarization must be used. In addition, our materials present flux of hydrogen by ambipolar diffusion of protons and electrons which additionally changes the gradient during measurement. However, one may emphasize that the partial conductivities calculated here should rather show the overall evolution of the different partial conductivities with temperature, which are, in turn, very well in accordance with what was expected from earlier reports [3,7,15].

Electrons are minority defects in both materials (concentration-wise), but due to their higher mobility, the conductivity is significant above a certain temperature: ~800 °C for LWO54, and ~600 °C for Mo-LWO54. The partial electronic conductivity can be estimated from pO_2 dependencies (Fig. 2), calculated as $\sigma_{e'} = \sigma_{\text{total}(5\%H_2)} + \sigma_{\text{ion(flat)}}$. These conductivities are compared in Fig. 6 with the ones extracted from the EMF method. The values are quite comparable between the two types of measurements, which confirm the consistency of the data. One may judge from the figure whether the electronic conductivity using the EMF method is slightly underestimated for Mo-LWO54, although the trends are the same, and the differences between the two are within the uncertainty of the EMF technique. Additionally, the comparison clearly shows that the electronic conductivity in Mo-LWO54 is about one order of magnitude higher than LWO54 in wet 5% H_2/Ar. The difference between LWO54 and Mo-LWO54 is even higher in H_2 since the electronic conductivity presents a strong dependence with oxygen partial pressure (c.f. Fig. 2). It is interesting to note that the protonic conductivity of LWO54 and Mo-LWO54 is quite similar when comparing the σ_{H^+} extracted from the transport number measurements, and the protonic conductivity is essentially the same at each temperature under both reducing and oxidizing conditions (see Fig. 7). This is in accordance with a concentration of ions being independent of pO_2 and determined by an electroneutrality condition typical of acceptor doped materials: $[Acc'] = 2[v_O^{\bullet\bullet}] + [OH_O^{\bullet}]$. It is therefore confirmed here that the electronic conductivity is enhanced substantially with Mo-substitution without altering the protonic conductivity significantly, as anticipated by Amsif et al. [15].

The protonic conductivity for LWO54 has been calculated according to an acceptor-doped model, i.e. a simplified version of the defect chemical model from Erdal et al. [7]. The "effective acceptor concentration" is determined from the concentration of inherently vacant oxygen sites in the lattice of the stoichiometric composition ($x = 0$, $La_{28}W_4O_{54}v_2$), and the exact La/W ratio, which determines the concentration of the defect $W_{La}^{\bullet\bullet\bullet}$. In our case, the composition is $La_{27}W_5O_{55.5}v_{0.5}$, so the "effective acceptor concentration" is

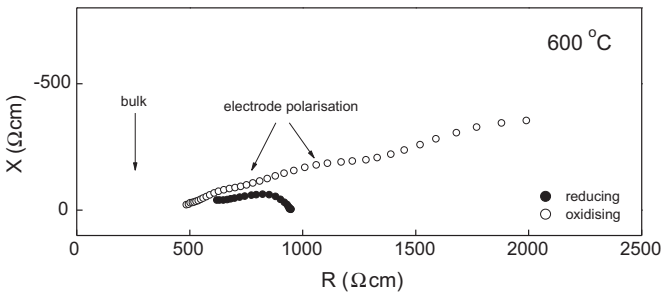

Fig. 4. Nyquist plot of LWO54 in reducing (5% H_2/Ar) or oxidizing (air) conditions under typical transport number measurement conditions (small chemical gradient across the sample).

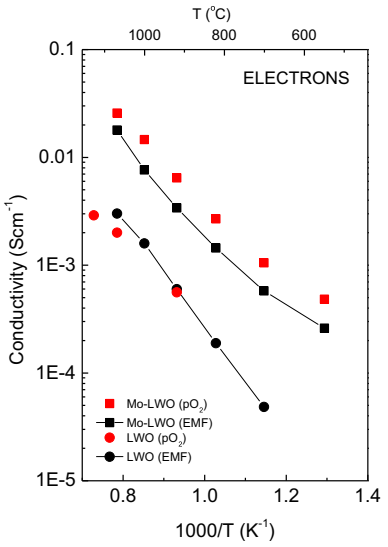

Fig. 6. Partial electronic conductivity in wet 5% H_2/Ar for LWO54 and Mo-LWO54 extracted from the EMF method (in black) and estimated from the dependency of conductivity with pO_2 from Fig. 2 (in red). (For interpretation of the references to color in this figure legend, the reader is referred to the web version of this article.)

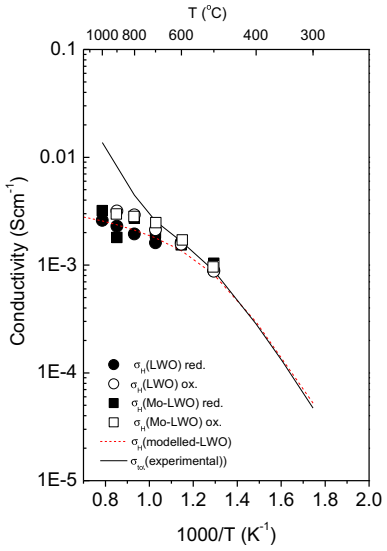

Fig. 7. Total (line) and partial protonic (symbols) conductivity extracted from the EMF method under reducing conditions for LWO54 and Mo-LWO54. The protonic conductivity has been modeled using the defect chemical model described in the text.

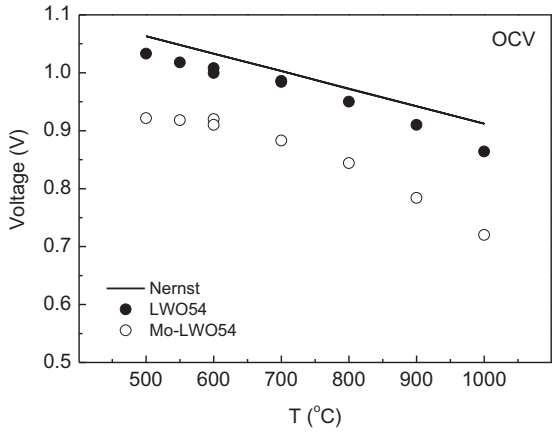

Fig. 8. Open circuit voltage of a Pt//(Mo)LWO//Pt fuel cell as a function of temperature. Gases: wet air (cathode) and wet 5% H_2/Ar (anode).

constant and written as: $[Acc^{/}]_{eff} = 2[v_O^{\bullet\bullet}] + [OH_O^{\bullet}] = 1$ (in mole fraction). Initial values for the thermodynamics of hydration of LWO54 were taken from Erdal et al. [7] and from independent thermogravimetric and combined TG-DSC measurements from Hancke et al. [8]. The data was fitted to $\Delta H_{m,H^+} \sim 63$ kJ mol^{-1} (0.65 eV), $\Delta H^0_{hydr} \sim -90$ kJ mol^{-1} and $\Delta S^0_{hydr} \sim -110$ J K^{-1} mol^{-1}, and the modeled partial proton conductivity is drawn in Fig. 7. The total conductivity is included to show the fit of the data at temperatures below 500 °C where the material is a pure proton conductor and the activation energy of migration of protons can be calculated. As evident, the modeled σ_{H^+} can reproduce quite reliably the trends shown by the experimental data, and the thermodynamic values in accordance with refs. [7,8].

3.3. Fuel cell testing of LWO54 and Mo-LWO54

After the transport number measurements were completed, the cell was run under fuel cell mode to check the performance of the materials. The variation of the open circuit voltage of LWO54 and Mo-LWO54 with temperature is plotted in Fig. 8. The OCV is very close to the theoretical one for LWO54, suggesting that ionic conductivity prevails over a large temperature range. The OCV changes from 98% of the Nernst voltage at 800 °C, 97% (at 900 °C) to 95% (at 1000 °C), which suggests that electronic conductivity starts to contribute, as confirmed by the EMF method described in section 3.2. On the other hand, the OCV of Mo-LWO54 is much lower than the theoretical, and lower than LWO54: 89% of the Nernst voltage at 800 °C, 83% (at 900 °C) to 79% (at 1000 °C), which clearly suggests that electronic conductivity is higher in the Mo-substituted material. This is very well in accordance with the transport numbers and partial conductivities extracted from the EMF method.

The performance of the cells as a function of temperature is shown in Fig. 9. Since the thickness was ~0.2 cm for both specimens, the current density and delivered maximum power can be directly compared. The performance of both materials increases with increasing temperature, in accordance with increasing ionic conductivity (protonic + oxide ion) with temperature. It is clear that LWO54 has a higher performance than Mo-LWO54, again in accordance with a higher OCV and higher dominance of ions over electrons/electron holes over the whole temperature range. The maximum power output is 13.6 mW cm^{-2} for LWO54, and 8.6 mW cm^{-2} for Mo-LWO54 at 1000 °C. At this temperature, the electrolyte is more of an oxide-ion conductor than protonic. The maximum power output is 0.4 mW cm^{-2} for LWO54, and 0.2 mW cm^{-2} for Mo-LWO54 at 500 °C. The ionic conductivity at this temperature reflects mainly protons.

It is therefore demonstrated in the present manuscript that LWO54 and Mo-LWO54 are mixed proton, oxide ion, n- and p-type conductors depending on temperature and atmosphere. Nominally undoped lanthanum tungstate is most suited for applications as electrolyte in proton conducting SOFCs, while Mo-LWO54

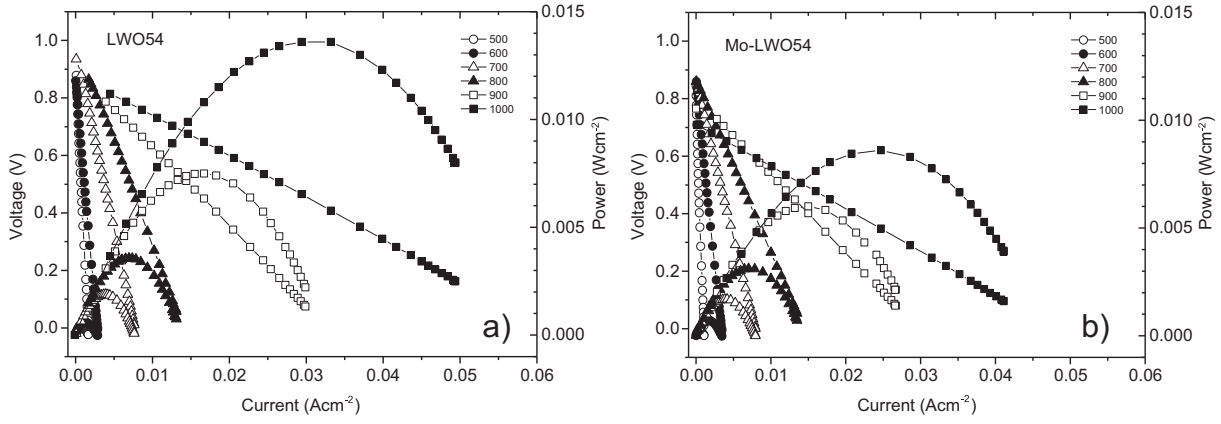

Fig. 9. Performance of the a) Pt//LWO54//Pt fuel cell and b) Pt//Mo-LWO54//Pt fuel cell as a function of temperature. Gases: wet air (cathode) and wet 5% H_2/Ar (anode).

potentially presents enhanced performance as a dense membrane for hydrogen separation.

4. Conclusions

Lanthanum tungstate ($La_{28-x}W_{4+x}O_{54+\delta}$ with $x = 1$) and 30% Mo-substituted lanthanum tungstate were investigated using the EMF method to extract the partial protonic, oxide ion and electronic conductivities. The measurements show that both materials are mixed proton-oxide ion-electron/electron hole conductors depending on temperature and atmospheric conditions. The manuscript confirms that molybdenum substitution in lanthanum tungstate increases the electronic conductivity by about one order of magnitude (in 5% H_2/Ar) while the protonic conductivity remains essentially unaffected. This makes LWO54 a good candidate as electrolyte in proton conducting SOFCs at intermediate temperatures and wet conditions, while Mo-LWO54 is more suited for application as a dense membrane for hydrogen separation.

Acknowledgments

The author wishes to thank support from the NaCo-SOFC project- “Nano Coatings for Solid Oxide Fuels Cells” funded by the Top-Level Research initiative and Ass. Prof. Reidar Haugsrud for fruitful discussions.

References

[1] A. Magrasó, J.M. Polfus, C. Frontera, J. Canales-Vazquez, L.-E. Kalland, C.H. Hervoches, S. Erdal, R. Hancke, M.S. Islam, T. Norby, R. Haugsrud, J. Mater. Chem. 22 (2012) 1762–1764.
[2] T. Shimura, S. Fujimoto, H. Iwahara, Solid State Ionics 143 (2001) 117–123.
[3] R. Haugsrud, Solid State Ionics 178 (2007) 555–560.
[4] R. Haugsrud, C. Kjølseth, J. Phys. Chem. Solids 69 (2008) 1758–1765.
[5] A. Magrasó, C. Frontera, D. Marrero-Lopez, P. Nunez, Dalton Trans. (2009) 10273–10283.
[6] M. Yoshimura, A. Rouanet, Mat. Res. Bull. 11 (1976) 151–158.
[7] S. Erdal, L.-E. Kalland, R. Hancke, J. Polfus, R. Haugsrud, T. Norby, A. Magrasó, Int. J. Hydrogen Energy 37 (2012) 8051–8055.
[8] R. Hancke, A. Magrasó, T. Norby, R. Haugsrud, Solid State Ionics 231 (2013) 25–29.
[9] A. Magrasó, C.H. Hervoches, I. Ahmed, S. Hull, J. Nordström, A.W.B. Skilbred, R. Haugsrud, J. Mater. Chem. A 1 (11) (2013) 3774–3782.
[10] C. Solis, L. Navarrete, S. Roitsch, J.M. Serra, J. Mater. Chem. 22 (2012) 16051–16059.
[11] E. Quarez, K.V. Kravchyk, O. Joubert, Solid State Ionics 216 (2012) 19–24.
[12] S. Erdal, Ph.D., University of Oslo, 2011.
[13] S. Escolastico, C. Solis, J.M. Serra, Solid State Ionics 216 (2012) 31–35.
[14] S. Escolastico, C. Solis, J.M. Serra, Int. J. Hydrogen Energy 36 (2011) 11946–11954.
[15] M. Amsif, A. Magrasó, D. Marrero-López, J.C. Ruiz-Morales, J. Canales-Vázquez, P. Núñez, Chem. Mater. 24 (20) (2012) 3868–3877.
[16] T. Norby, Solid State Ionics 28-30 (1988) 1586–1591.
[17] T. Norby, P. Kofstad, J. Am. Ceram. Soc. 67 (1984) 786–792.
[18] M. Liu, H. Hu, J. Electrochem. Soc. 143 (6) (1996) L109–L112.
[19] C. Wagner, Z. Physik. Chem. (B) 21 (1933) 25.
[20] D.P. Sutija, T. Norby, P. Björnbom, Solid State Ionics 77 (1995) 167.
[21] M. Widerøe, R. Waser, T. Norby, Solid State Ionics 177 (2006) 1469–1476.